

Single Particle Stochastic Heat Engine

Shubhashis Rana¹, P. S. Pal¹, Arnab Saha², A. M. Jayannavar^{1*}

Institute of Physics, Sachivalaya Marg, Bhubaneswar - 751005, India¹

Institut für Theoretische Physik II, Weiche Materie,

Heinrich-Heine-Universität Düsseldorf, 40225 Düsseldorf, Germany²

We have performed an extensive analysis of a single particle stochastic heat engine constructed by manipulating a Brownian particle in a time dependent harmonic potential. The cycle consists of two isothermal steps at different temperatures and two adiabatic steps similar to that of a Carnot engine. The engine shows qualitative differences in inertial and overdamped regimes. All the thermodynamic quantities, including efficiency, exhibit strong fluctuations in a time periodic steady state. The fluctuations of stochastic efficiency dominate over the mean values even in the quasistatic regime. Interestingly, our system acts as an engine provided the temperature difference between the two reservoirs is greater than a finite critical value which in turn depends on the cycle time and other system parameters. This is supported by our analytical results carried out in the quasistatic regime. Our system works more reliably as an engine for large cycle times. By studying various model systems we observe that the operational characteristics are model dependent. Our results clearly rules out any universal relation between efficiency at maximum power and temperature of the baths. We have also verified fluctuation relations for heat engines in time periodic steady state.

PACS numbers: 05.40.Jc, 05.40.-a, 05.70.Ln

Keywords: Heat engines, stochastic efficiency, fluctuations

I. INTRODUCTION

Thermodynamic heat engines convert heat into useful work. They work cyclically between two thermal reservoirs kept at different temperatures T_l and T_h ($T_h > T_l$). The Second law of thermodynamics restricts their efficiency to the Carnot limit [1], $\eta_C = 1 - \frac{T_l}{T_h}$. However, this efficiency can only be achieved in the quasistatic limit where transitions between thermodynamic states occur infinitesimally slowly and hence the power output vanishes. Curzon and Ahlborn (C-A) [2] showed that for finite time endoreversible heat engines, efficiency at maximum power is given by $\eta_{CA} = 1 - \sqrt{\frac{T_l}{T_h}}$. As yet there is no consensus on this result ([3–7]).

With the advances in nano-technology, a few-micrometer-sized Stirling heat engine has been experimentally realized [8]. This microscopic heat engine operates in conditions where typical changes in their energies are of the order of the thermal energy per degree of freedom [9]. An appropriate theoretical framework to deal with these systems has been developed during the past decades within the context of stochastic thermodynamics [10–14]. This formalism of stochastic energetics provides a method to calculate work, heat and entropy even for a single particle along a microscopic trajectory. One can obtain average quantities after averaging over respective ensembles. The averaged thermo-

dynamic quantities, work and entropy, obey Second law. Using this formulation various single particle heat engines have been studied in the literature [4, 15–18]. Fluctuation relations for heat engines (FRHE) [19–21] operating in a time periodic steady state (TPSS) have recently been obtained [20]. FRHE are in the form of equality and Carnot's inequality for efficiency η_c follows as a direct consequence of this theorem.

In the present work we have studied in detail a simple model for a stochastic heat engine described by Langevin equation. Both underdamped and overdamped regimes are explored and qualitative differences are pointed out. We emphasize on fluctuations of thermodynamic variables including the engine efficiency. We show that fluctuations dominate the mean values even in quasistatic regime. Therefore in such situations one needs to study the full probability distribution of the physical variable for the proper analysis of the system.

In section II, we describe the model of our system and the protocol. In section III, we obtain analytical results for relevant average thermodynamic quantities in the quasistatic regime for the underdamped case. In section IV, engine with finite time cycle in the inertial regime is studied numerically, in detail. The system driven by time asymmetric cycles and various other model systems are also explored. We have verified FRHE in this section. Sections V and VI are devoted to the analytical and numerical studies of the system in the overdamped limit. Finally, we conclude in section VII. Each section is self contained.

*Electronic address: shubho@iopb.res.in, priyo@iopb.res.in, saha@iopb.res.in, ajay@iopb.res.in

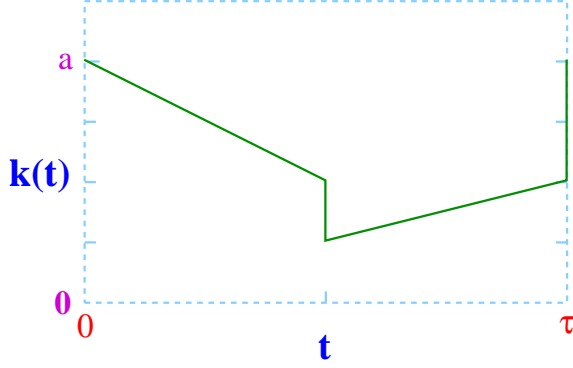


FIG. 1: (Color online) Stochastic heat engine in a harmonic potential: the time dependence of our periodically driven stiffness constant (protocol) $k(t)$ for the full cycle ($0 \leq t \leq \tau$).

II. THE MODEL

The single particle stochastic heat engine consists of a Brownian particle having position x and velocity v at time t , confined in a one dimensional harmonic trap. The stiffness of the trap $k(t)$ varies periodically in time as shown in Fig.(1). For the underdamped case, the equation of motion for the particle is given by [22, 23]

$$m\dot{v} = -\gamma v - k(t)x + \sqrt{\gamma T}\xi(t). \quad (1)$$

In overdamped limit the equation reduces to

$$\gamma\dot{x} = -k(t)x + \sqrt{\gamma T}\xi(t). \quad (2)$$

In our further analysis, we set mass of the particle m , the Boltzmann constant k_B and the frictional coefficient γ to be unity. T is the temperature of the thermal bath. All physical parameters are made dimensionless. The noise is Gaussian with zero mean, $\langle \xi(t) \rangle = 0$ and is delta correlated, $\langle \xi(t_1)\xi(t_2) \rangle = 2\delta(t_1 - t_2)$. The internal energies of the particle in the underdamped and the overdamped limit are given by $u(x, v) = \frac{1}{2}k(t)x^2 + \frac{1}{2}mv^2$ and $u(x) = \frac{1}{2}k(t)x^2$, respectively.

Operation of the system consists of four steps - two isotherms and two adiabatics. In the first step, the system undergoes an isothermal expansion, during which it is connected to a hot bath at temperature T_h and the stiffness constant is varied linearly with time as

$$k(t) = a \left(1 - \frac{t}{\tau}\right) = k_1(t) \quad (3)$$

for $0 < t < \tau/2$. Here τ is the period of the cycle and a is the initial value of the stiffness constant.

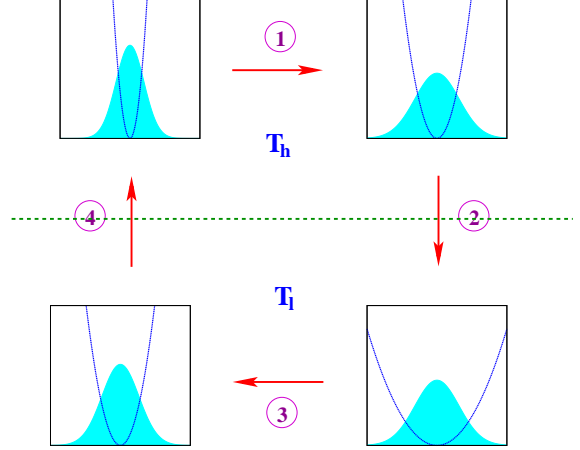


FIG. 2: (Color online) Schematic representation for a cyclic process of stochastic heat engine operating between two reservoirs kept at temperatures T_h and T_l . The cycle consists of two isothermal steps and two adiabatic steps according to the time varying protocol $k(t)$. The blue line denotes a one dimensional potential $V(x,t)$ and the filled region denote the corresponding steady state distribution.

In the second step, the potential undergoes an instantaneous expansion (adiabatic) by decreasing the stiffness constant from $a/2$ to $a/4$. As the process is instantaneous the distribution before and after expansion will not change and heat absorption will be zero. In the third step, the system is connected to a cold bath with lower temperature T_l and isothermal compression of the trap is carried out by changing the stiffness as

$$k(t) = a \frac{t}{2\tau} = k_2(t) \quad (4)$$

for $\tau/2 < t < \tau$. In the last step, we carry out instantaneous adiabatic compression by varying the stiffness constant from $a/2$ to a and simultaneously connecting the system to the hot bath. This cycle is then repeated. The time dependence of the protocol is given in Fig.(1) and a schematic representation of the system within a cycle at its various stages is depicted in Fig.(2).

The described protocol differs from those used in earlier studies. In the experimental set up [8] two adiabatic steps are absent. Work optimized protocol is used by Schmiedl and Seifert [4] whereas the protocol based on the concept of shortcut to adiabaticity is used by Tu [16]. However, their emphasis is on the possible correlation between efficiency at maximum power and C-A bound. Our main motivation, namely to study the fluctuation of physical quantities, is different from earlier studies as mentioned in the introduction.

III. UNDERDAMPED QUASISTATIC LIMIT

In this section, we analytically calculate the average thermodynamic quantities of our model system in the quasistatic limit. In this limit, the duration of the protocol is much larger than all the relevant time scales, including the relaxation time. Hence as protocol is changed, the system immediately adjusts to the equilibrium state corresponding to the value of protocol at that instant. First, we calculate the average work done on the particle in all the four steps of a cycle and the heat absorbed by it in the first isothermal step. Finally, we calculate efficiency in the quasistatic limit.

In the first isothermal process, average work done on the particle is the same as the free energy change (ΔF_h) before and after the expansion, i.e.,

$$W_1 = \Delta F_h = \frac{T_h}{2} \ln \frac{k_1(\tau/2)}{k_1(\tau)} = \frac{T_h}{2} \ln \frac{1}{2}. \quad (5)$$

At $t = \tau/2$, the system is in equilibrium with the bath at T_h with stiffness constant $a/2$. The second step being instantaneous, no heat will be dissipated and the phase space distribution remains unaltered. Correspondingly the average work done on the particle is equal to the change in its internal energy:

$$\begin{aligned} W_2 &= N_1 \int_{-\infty}^{\infty} dx dv \left(\frac{a}{4} - \frac{a}{2} \right) \frac{x^2}{2} e^{-\frac{ax^2}{4T_h} - \frac{v^2}{2T_h}} \\ &= -\frac{T_h}{4}, \end{aligned} \quad (6)$$

where $N_1 = \frac{1}{2\pi T_h} \sqrt{\frac{a}{2}}$, is the normalization constant. Similarly in the third step (i.e., isothermal compression step) the average work done on the particle in the quasistatic limit is

$$W_3 = \Delta F_l = \frac{T_l}{2} \ln \frac{k_2(\tau)}{k_2(\tau/2)} = \frac{T_l}{2} \ln 2. \quad (7)$$

The average work done in the last step (i.e., second adiabatic step) is given as

$$\begin{aligned} W_4 &= N_2 \int_{-\infty}^{\infty} dx dv \left(a - \frac{a}{2} \right) \frac{x^2}{2} e^{-\frac{ax^2}{4T_l} - \frac{v^2}{2T_l}} \\ &= \frac{T_l}{2}, \end{aligned} \quad (8)$$

with $N_2 = \frac{1}{2\pi T_l} \sqrt{\frac{a}{2}}$. Hence, the average total work done in the full cycle of the heat engine in the quasistatic process is

$$\begin{aligned} W_{tot} &= W_1 + W_2 + W_3 + W_4 \\ &= \frac{T_h}{2} \ln \frac{1}{2} - \frac{T_h}{4} + \frac{T_l}{2} \ln 2 + \frac{T_l}{2}. \end{aligned} \quad (9)$$

To obtain the heat absorption in the first step (i.e., isothermal expansion), we calculate the average change of internal energy and use the First law. During this process, the particle stays in contact with hot bath at temperature T_h . However, it is to be noted that at time $t = 0^-$, the system was in contact with low temperature bath at T_l , whereas at $t = 0^+$ the system is in contact with hot bath at T_h . Thus the system has to relax into new equilibrium after sudden change in temperature. The time taken for this relaxation process is assumed to be negligible compared to the cycle time τ . This relaxation leads to an additional heat flow which accounts for the change in the internal energy during the relaxation process. One can readily obtain the internal energy at $t = 0^+$ as $3T_l/2$ while after the relaxation it is T_h . Hence, the average internal energy change in the first step is

$$\Delta U_1 = T_h - \frac{3T_l}{2}. \quad (10)$$

Now using the First law, the average heat absorption from the hot bath for the first step is

$$-Q_1 = \Delta U_1 - W_1 = T_h - \frac{3T_l}{2} - \frac{T_h}{2} \ln \frac{1}{2}. \quad (11)$$

Hence efficiency of the engine for the underdamped case in the quasistatic limit is given by

$$\begin{aligned} \bar{\eta}_q &= \frac{-W_{tot}}{-Q_1} = -\frac{\frac{T_h}{2} \ln \frac{1}{2} - \frac{T_h}{4} + \frac{T_l}{2} \ln 2 + \frac{T_l}{2}}{T_h - \frac{3T_l}{2} - \frac{T_h}{2} \ln \frac{1}{2}} \\ &= -\frac{T_h \ln \frac{1}{2} - \frac{T_h}{2} + T_l \ln 2 + T_l}{2T_h - 3T_l - T_h \ln \frac{1}{2}}. \end{aligned} \quad (12)$$

Here we would like to emphasize that $\bar{\eta}$ is defined ignoring fluctuations and the subscript q denotes the quasistatic limit. We will show later that fluctuations play an important role even in the quasistatic regime. Work done during the cycle w and heat absorbed during the first step q_1 are fluctuating quantities. Stochastic efficiency is defined as $\eta = \frac{w}{q_1}$ [18] and hence its average $\langle \eta \rangle = \langle \frac{w}{q_1} \rangle$ is not the same as $\bar{\eta} = \frac{\langle w \rangle}{\langle q_1 \rangle}$ which is given in Eq.(12) for quasistatic limit. This will be discussed in detail in subsequent sections. In our notation, the thermodynamic quantities are denoted by capital letters only for quasistatic limit, whereas, small letters are used to denote those quantities for finite time cycles.

According to our convention negative work done on the system implies extraction of work; while, negative heat means that heat enters into the system. It is important to note from Eq.(11) that in quasistatic limit heat flows from the bath to the

system provided

$$2T_h - 3T_l - T_h \ln \frac{1}{2} \geq 0$$

$$\Rightarrow \frac{T_l}{T_h} \leq \frac{2 + \ln 2}{3} = 0.898 \quad (13)$$

and similarly from Eq.(9) work can be extracted from the system if

$$T_h \ln \frac{1}{2} - \frac{T_h}{2} + T_l \ln 2 + T_l \leq 0$$

$$\Rightarrow \frac{T_l}{T_h} \leq \frac{0.5 + \ln 2}{1 + \ln 2} = 0.705. \quad (14)$$

Therefore, in quasistatic regime our model system operates in three different modes of operation depending on the ratio of the temperatures of the thermal baths. First, when $0 < \frac{T_l}{T_h} \leq 0.705$ is maintained, work can be extracted and heat is absorbed from hot bath and it acts as an engine. Second, when $0.705 \leq \frac{T_l}{T_h} \leq 0.898$ is set, heat is absorbed from the bath but we cannot extract work. And finally when we have $\frac{T_l}{T_h} \geq 0.898$ neither heat is absorbed nor the work is extracted. In this case work done on the system heats up the hot bath. Therefore, there is a particular regime in parameter space where the system act as an engine. This is in contrast to the Carnot engine which works for arbitrary temperature difference between two baths. The above mentioned condition is only valid in the quasistatic limit. For finite time cycle the operational condition for heat engine depends on cycle time apart from T_h and T_l , which will be shown in our simulation. Our exact expression of W_{tot} and Q_1 are in complete agreement with our numerical results in the quasistatic limit. Thus these analytical calculations act as a check for our numerical simulation.

IV. FINITE CYCLE TIME ENGINE IN INERTIAL REGIME

For finite-cycle-time we study our system numerically. When the Langevin system is driven periodically it is known that after initial transients, the system will settle down to a TPSS. The joint probability distribution $P_{ss}(x, v, t)$ of position and velocity of the particle is periodic in time, i.e., $P_{ss}(x, v, t) = P_{ss}(x, v, t + \tau)$.

For numerical simulations we evolve our system with a time periodic protocol (as shown in Fig.1). We have used Heun's method for integrating the basic Langevin equation [24] with time step $dt = 0.0002$. We make sure that the system is in the TPSS by going beyond the initial transient regime. We then consider at least 10^5 cycles of operations and physical quantities are averaged over all these

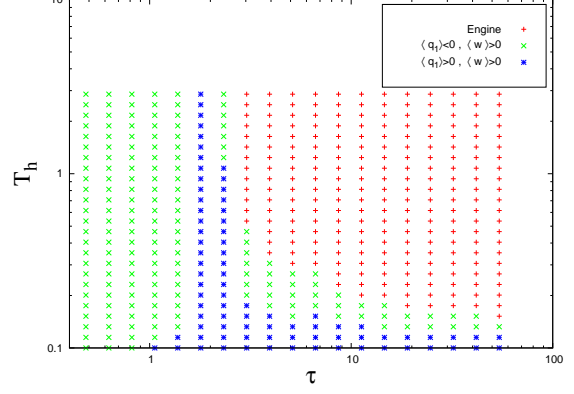


FIG. 3: (Color online) Phase diagram for different T_h and τ but for fixed $T_l = 0.1$.

cycles. For rest of the paper we keep m, a, γ fixed at $m = 1.0, a = 5.0, \gamma = 1.0$.

We now make use of the concepts of stochastic energetics [10–14] to calculate work, heat and internal energy for a given trajectory. The thermodynamic work done on the particle during first part of the cycle, in each computational step dt , is given by

$$dw_1(t_i) = \frac{\partial u_1(t_i)}{\partial k_1(t_i)} \dot{k}_1(t_i) dt. \quad (15)$$

with $u_1(t_i) = \frac{1}{2}k_1(t_i)x^2(t_i) + \frac{1}{2}v^2(t_i)$ and $t_i = i \cdot dt$. Now, $w_1 = \sum_{i=0}^N dw_1(t_i)$ where $N = \frac{\tau}{2dt}$. The internal energy is a thermodynamic state function and hence its change during the isothermal process is given by $du_1 = \frac{1}{2}k_1(\tau/2)x^2(\tau/2) + \frac{1}{2}v^2(\tau/2) - \frac{1}{2}k_1(0)x^2(0) - \frac{1}{2}v^2(0)$. The heat absorption by the bath is $q_1 = w_1 - du_1$ using the First law of thermodynamics. The second step which is adiabatic is instantaneous and hence the particle does not get any chance to evolve. Thus work done is only instantaneous change in internal energy, i.e., $w_2 = \frac{1}{2}[k_2(\tau/2) - k_1(\tau/2)]x^2(\tau/2)$. Similarly, for step three, work done is given by

$$dw_3(t_i) = \frac{\partial u_2(t_i)}{\partial k_2(t_i)} \dot{k}_2(t_i) dt \quad (16)$$

and $w_3 = \sum_{i=N}^{2N} dw_3(t_i)$; internal energy change $du_2 = \frac{1}{2}k_2(\tau)x^2(\tau) + \frac{1}{2}v^2(\tau) - \frac{1}{2}k_2(\tau/2)x^2(\tau/2) - \frac{1}{2}v^2(\tau/2)$; and heat delivered to the cold bath is $q_2 = w_3 - du_2$. For the last adiabatic process, work done on the particle is $w_4 = \frac{1}{2}[k_1(0) - k_2(\tau)]x^2(\tau)$. The total work done on the system in a cycle is $w = w_1 + w_2 + w_3 + w_4$. It should be noted that each w_i ($i=1,2,3,4$) is a fluctuating quantity and their values depend on a particular phase space trajectory.

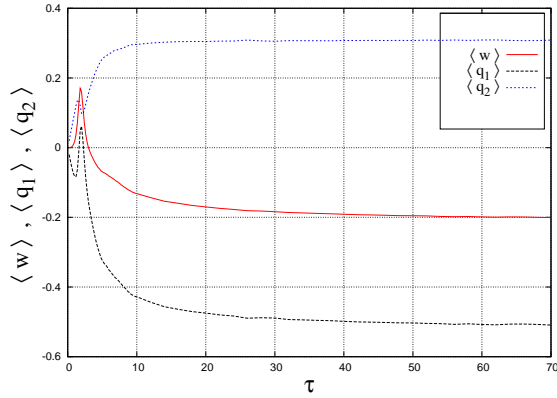


FIG. 4: (Color online) Variation of $\langle w \rangle$, $\langle q_1 \rangle$ and $\langle q_2 \rangle$ with cycle time τ .

In Fig.(3), we have shown the phase diagram of the operation of our system. Here we have varied T_h and cycle time τ keeping T_l fixed at 0.1. There are three distinct regimes. The system acts as an engine when $\langle w \rangle < 0$ and $\langle q_1 \rangle < 0$. The angular bracket $\langle \cdot \rangle$ indicates average over several realizations. In the other two regimes the system ceases to work as a heat engine altogether ($\langle w \rangle > 0$). For $\langle w \rangle > 0$ we have two distinct domains with $\langle q_1 \rangle < 0$ and $\langle q_1 \rangle > 0$. The latter implies work is done on the system which heats up the hot bath. In the large cycle time limit numerical results are consistent with our analytical predictions made in last section. We re-emphasize that the system works as a heat engine provided there is a minimal difference between T_h and T_l which depends on cycle time τ and other physical parameters. From the Phase diagram it is apparent that, as we decrease τ for fixed T_h , there exists a lower bound below which the system does not perform as an engine, as it only consumes work.

In Fig.(4), we have plotted $\langle w \rangle$, $\langle q_1 \rangle$ and $\langle q_2 \rangle$ with respect to cycle time τ . We have fixed $T_h = 0.5$ and $T_l = 0.1$ for all subsequent figures. Starting from zero, $\langle w \rangle$ initially increases and reaches a peak value. Then it starts decreasing and finally saturates to a negative value (-0.214), which is close to our theoretical result (from Eq.(9)). The work can be extracted in the region where it becomes negative. As we increase cycle time, $\langle q_1 \rangle$ changes dramatically. It has a positive region sandwiched between two negative regions. When $\langle q_1 \rangle > 0$ heat is released to the hot bath while work is done on the particle. In the quasistatic limit it saturates at the theoretical value -0.523 (from Eq.(11)). In contrast to $\langle q_1 \rangle$, $\langle q_2 \rangle$ is always positive, i.e., heat is always released to the cold bath. Internal energy being a state function, $\langle \Delta u \rangle$ is zero over a cycle in TPSS and hence $\langle w \rangle = \langle q_1 \rangle + \langle q_2 \rangle$.

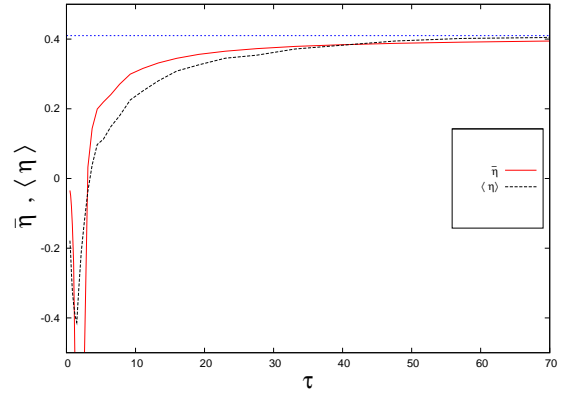


FIG. 5: (Color online) Variation of $\langle \eta \rangle$ and $\bar{\eta}$ with cycle time τ . The dotted blue line denotes the quasistatic limit for $\bar{\eta}$.

Using the saturation value of $\langle w \rangle$ and $\langle q_1 \rangle$ we immediately get $\langle q_2 \rangle$ to be equal to 0.310 which is close to our numerical result.

We now study the nature of stochastic efficiency η and engine power $p = -\frac{w}{\tau}$ as a function of cycle time. The engine is in TPSS where probability distributions of system variables are periodic in time. However, for a given realization of a cycle, state of the system (position and velocity) does not come back to its initial state. Thus for each cycle thermodynamic quantities will depend on the particular microscopic trajectory and hence w , q_1 , q_2 , η and p are all fluctuating quantities from cycle to cycle. The average efficiency is defined as $\langle \eta \rangle = \langle \frac{w}{q_1} \rangle$. Due to fluctuation in w and q_1 , it is to be noted that $\langle \eta \rangle = \langle \frac{w}{q_1} \rangle \neq \frac{\langle w \rangle}{\langle q_1 \rangle} = \bar{\eta}$. Fluctuation theorems [19–21] put stringent condition on $\frac{\langle w \rangle}{\langle q_1 \rangle}$ which is bounded by the Carnot efficiency i.e., $\frac{\langle w \rangle}{\langle q_1 \rangle} \leq 1 - \frac{T_l}{T_h}$. However, no such bound exist for $\langle \eta \rangle$ [21].

The First law for any microscopic realization of cycle can be written as

$$w = \Delta u + q_1 + q_2. \quad (17)$$

The change in the internal energy Δu is unbounded. It is zero only on the average. Similarly q_1, q_2 and w take values in the range $(-\infty, \infty)$ but are constrained by First law. Hence it is not surprising that η can take values between $-\infty$ to ∞ .

In Fig.(5) we have plotted efficiencies $\langle \eta \rangle$ and $\bar{\eta}$ as a function of cycle time. Initially for small τ , our system doesn't work as an engine. Due to large dissipation work cannot be extracted ($\langle w \rangle \geq 0$). In this regime, efficiency is negative. On further increasing τ , efficiency becomes positive and it monotonically increases. For large τ , $\langle \eta \rangle$ and $\bar{\eta}$ saturate. The saturation value for $\bar{\eta}$ is 0.41 which

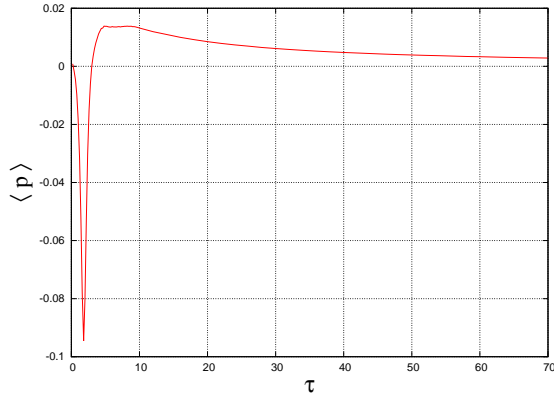


FIG. 6: (Color online) Variation of average power $\langle p \rangle$ with cycle time τ .

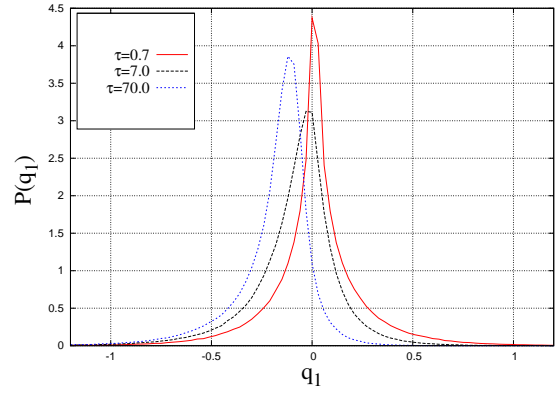


FIG. 8: (Color online) Distribution of q_1 for different cycle times.

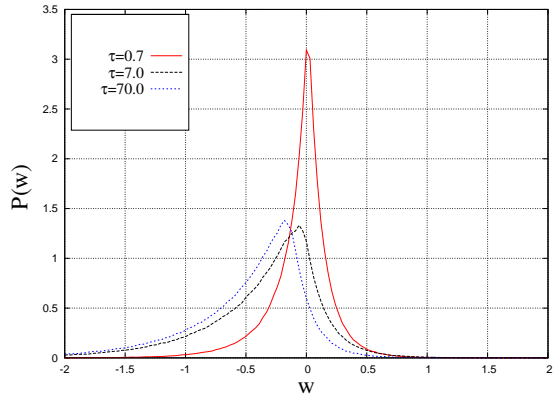


FIG. 7: (Color online) Distribution of w for different cycle times ($\tau=0.7, 7.0, 70.0$).

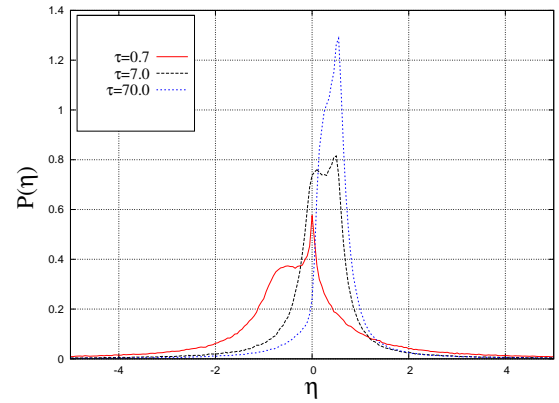


FIG. 9: (Color online) Distribution of η for different cycle times.

can be obtained analytically in quasistatic regime. In general $\langle \eta \rangle \neq \bar{\eta}$. We find both $\langle \eta \rangle$ and $\bar{\eta}$ are less than the Carnot efficiency $\eta_c = 0.8$.

In Fig.(6), average power $\langle p \rangle$ is plotted as a function of τ . There is a negative region for low cycle time. Beyond the critical value of $\tau \simeq 3.0$, power becomes positive and exhibits a peak and finally tends to zero in the large τ limit. The efficiencies $\langle \eta \rangle$ and $\bar{\eta}$ at maximum power are given by 0.16 and 0.25 respectively. Both of these values are less than $\eta_{CA} = 0.554$.

As mentioned earlier, physical quantities q_1 , w and η are strongly fluctuating variables. To study these fluctuations we focus on probability distribution of these quantities $P(q_1)$, $P(w)$ and $P(\eta)$. In figs.(7), (8) and (9) we have plotted them for three different time periods. For $\tau = 0.7$, distribution of w and q_1 are sharply peaked around zero with $\langle w \rangle = 0.005$, $\langle q_1 \rangle = -0.065$. As we increase the cycle time $P(w)$ and $P(q_1)$ become broad, asymmetric and shift towards negative side. For large

negative value of arguments the distributions exhibit long tail. For large positive values of w and q_1 the distribution falls off exponentially or faster [25]. The trajectory responsible for positive values are atypical and sometimes referred to as transient Second law violating trajectories [26–28]. Strong fluctuations in heat and work persist even in the quasistatic limit ($\tau = 70$). These fluctuations in work are mainly attributed to two adiabatic processes, while fluctuations of q_1 result from relaxation process when the system, in contact with low temperature bath, is brought in direct contact with high temperature reservoir.

For $\tau = 0.7$, $\langle \eta \rangle$ is negative (-0.26). The distribution $P(\eta)$ is asymmetric and there is a broad shoulder on the negative side. As we increase τ , distribution shifts towards positive side. It is not surprising to see the finite weight for values $\eta < 0$ and $\eta > 1$ [21]. As we increase the cycle time the standard deviation of η (σ_η), becomes smaller. However, it remains larger compared to mean val-

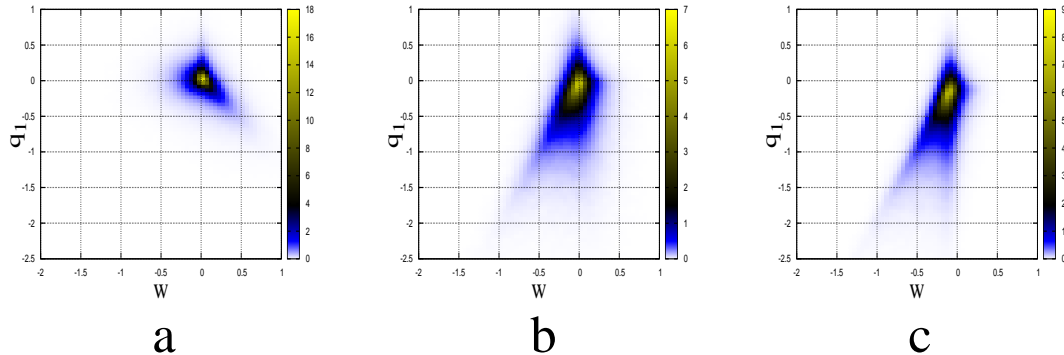


FIG. 10: (Color online) Joint distribution of w and q_1 for different τ . In a) $\tau = 0.7$, in b) $\tau = 7.0$, in c) $\tau = 70$.

ues. For example, $\langle \eta \rangle = 0.161$ and corresponding $\sigma_\eta = 1.32$ at $\tau = 7.0$ and $\langle \eta \rangle = 0.406$ whereas $\sigma_\eta = 1.11$ for $\tau = 70.0$. We would like to emphasize that mean is dominated by fluctuations even in the quasistatic regime. Any physical quantity with relative variance larger than one, is referred to as non-self averaging quantity. For such cases mean ceases to be a good physical variable and one has to resort to the analysis for full probability distribution. This is one of our main result. Non-self averaging quantities arises mainly in physics of quenched disordered systems.

Note that, η becomes positive if both w and q_1 are positive or both of them are negative. η becomes negative when w and q_1 have opposite signs. In order to have a better understanding of our system we have plotted the joint distributions of w and q_1 for different τ in Fig.(10). For a given cycle, the system acts as an engine when both w and q_1 are negative i.e., in the third quadrant of the plot. Using our numerical results we have calculated the ratio of the total number of realizations falling in the third quadrant to the total number of realizations. These fractions for $\tau = 0.7$, 7.0 and 70.0 are calculated to be 0.226 , 0.583 and 0.858 , respectively. It is clear from this that for large cycle times the reliability of the system working as an engine increases. Though we observe that even in quasistatic regime there are realizations for which the system does not act as an engine. This is due to strong fluctuations in work and heat as discussed earlier.

In TPSS the joint probability density $P_{ss}(x, v, t)$ is periodic in time: $P_{ss}(x, v, t + \tau) = P_{ss}(x, v, t)$. For simplicity we write $P_{ss}(x, v, t) = e^{-\phi(x, v, t)}$. From the definition of stochastic entropy [29–31] of the system S_{sys} , the change in the system entropy for a trajectory over a cycle is given by $\Delta S_{sys} = \Delta \phi = \phi(x_2, v_2, \tau) - \phi(x_1, v_1, 0)$ where (x_1, v_1) and (x_2, v_2) are the initial and final phase

space points for a particular realization of the cycle. To calculate $\Delta \phi$ we evaluate $P_{ss}(x, v, 0)$ at the initial point of the cycle which also coincide at the end point $t = \tau$. In Fig.(11) we have plotted joint phase space distribution at TPSS for three different values of $\tau = 0.7$, 7.0 and 70.0 . We see that for $\tau = 0.7$ and $\tau = 7.0$ phase space distributions are not symmetric and there exist strong correlation between x and v which was ignored in the earlier literature [16]. Only in the large τ limit the distribution becomes symmetric (see Fig.(11c)). The cross-correlation between position and velocity disappears and the distribution $P_{ss}(x, v)$ becomes uncorrelated Gaussian in the quasistatic limit. Due to correlation, the width of the distribution become larger as we decrease cycle time τ .

Recently, FRHE in TPSS has been derived [20]. It extends the total entropy production fluctuation theorem of Seifert [29, 30, 32] applied to heat engine. The total entropy production ΔS_{tot} over a cycle is a stochastic variable and in our present case is given by

$$\Delta S_{tot} = \Delta \phi + \frac{q_1}{T_h} + \frac{q_2}{T_l}. \quad (18)$$

Using the First law (Eq.17)

$$\Delta S_{tot} = \Delta \phi + \frac{q_1}{T_h} + \frac{w - q_1 - \Delta u}{T_l}. \quad (19)$$

The Second law which is valid on average, can be stated as $\langle \Delta S_{tot} \rangle \geq 0$. In TPSS, $\langle \Delta u \rangle = \langle \Delta \phi \rangle = 0$, which implies $\bar{\eta} = \frac{\langle w \rangle}{\langle q_1 \rangle} \leq 1 - \frac{T_l}{T_h} = \eta_c$. Thus the Second law puts the constraint on efficiency which is defined as $\frac{\langle w \rangle}{\langle q_1 \rangle}$. It should be noted that this constraint is valid for any finite time cycle in TPSS, unlike the Carnot which is valid for macroscopic engines in the quasistatic regime. However,

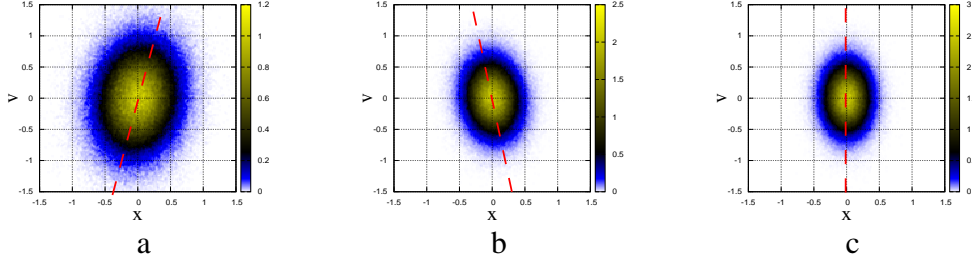


FIG. 11: (Color online) Initial phase space distribution at different cycle times τ . In a) $\tau = 0.7$, in b) $\tau = 7.0$, in c) $\tau = 70$. The asymmetric position of red broken line along the major axis of the elliptical Gaussian distribution for lower values of τ ($=0.7$ and 7.0) indicates nonzero $\langle xv \rangle$. This correlation becomes zero for larger τ ($=70$), where the position of the major axis also becomes symmetric.

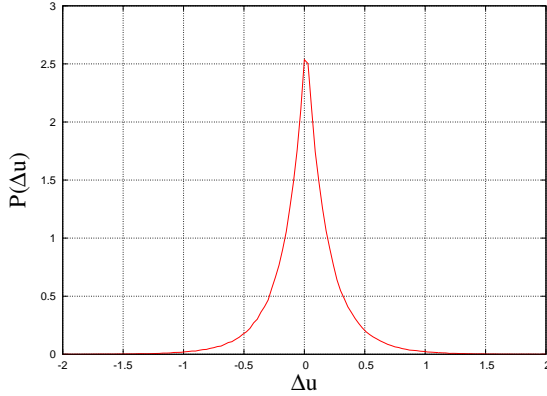


FIG. 12: (Color online) Distribution of the internal energy change in one cycle for underdamped steady state for $\tau = 7.0$.

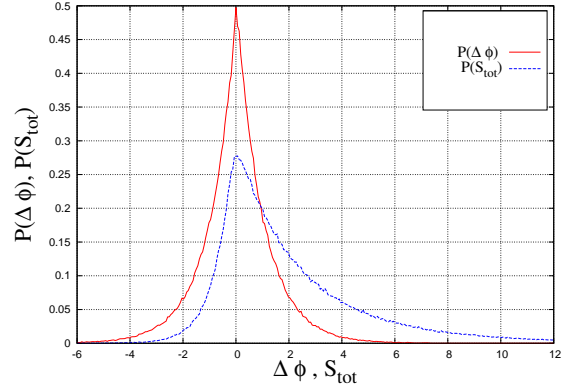


FIG. 13: (Color online) Distribution of system entropy change and total entropy production in one cycle for underdamped steady state for $\tau = 7.0$.

it does not put any constraint on the average efficiency ($\langle \frac{w}{q_1} \rangle$). The fluctuation theorem for heat engine replaces the inequality relation of the Second law by the equality relation, namely [20],

$$\langle e^{-\Delta S_{tot}} \rangle = \langle e^{-(\Delta\phi + \frac{q_1}{T_h} + \frac{w - q_1 - \Delta u}{T_l})} \rangle = 1 \quad (20)$$

Eq.(20) is FRHE in TPSS. By calculating all the relevant stochastic variables w , q_1 , $\Delta\phi$, Δu over all trajectories for finite τ we have verified Eq.(20) in the TPSS. We have obtained the value to be 0.96 for $\tau = 7.0$, which is well within our numerical accuracy. We would like to emphasize that, in Eq.(20), four stochastic variables appear in the exponent. Small changes in these values affect the exponential function by a large amount. Given this fact, our observed value of $\langle e^{-\Delta S_{tot}} \rangle$ is quite satisfactory.

For the same parameter value $\tau = 7.0$, in Fig.(12) we have plotted the probability distribution, $P(\Delta u)$, as a function of Δu . In Fig.(13),

we have plotted the probability distribution of change of system entropy $P(\Delta\phi)$ and total entropy $P(\Delta S_{tot})$ as a function of their arguments. It is clear that as u and ϕ are state functions, $P(\Delta u)$ and $P(\Delta\phi)$ are symmetric with zero mean. However, the distribution $P(\Delta S_{tot})$ is asymmetric with a long tail for positive large ΔS_{tot} . There is also a finite weight towards negative ΔS_{tot} . This contribution arises due to transient Second law violating periodic cycles [26, 28]. However, $\langle \Delta S_{tot} \rangle$ remains positive as demanded by the Second law.

Till now we concentrated on symmetric cycle, i.e., equal contact times of the system with hot and cold bath. Naturally, the question arises what will happen if the cycle is time asymmetric. To the best of our knowledge this question has not been addressed in earlier literature. If the contact time of one bath is different from that of the other, it can affect work output, heat dissipation to each bath, power and efficiency. However, in

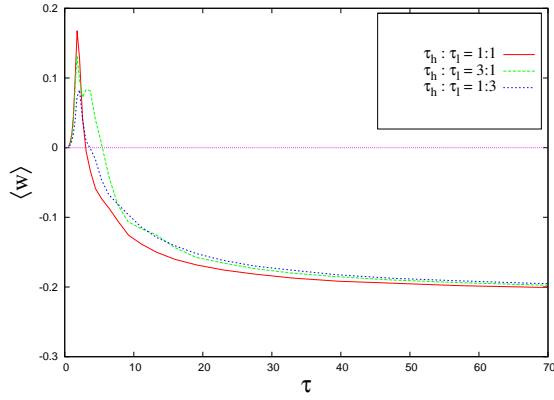


FIG. 14: (Color online) Variation of $\langle w \rangle$ vs τ for symmetric as well as asymmetrical cycles. Here τ_h and τ_l are contact times of the particle with hot and cold bath respectively. Thus, $\tau = \tau_h + \tau_l = 7.0$ for our case.

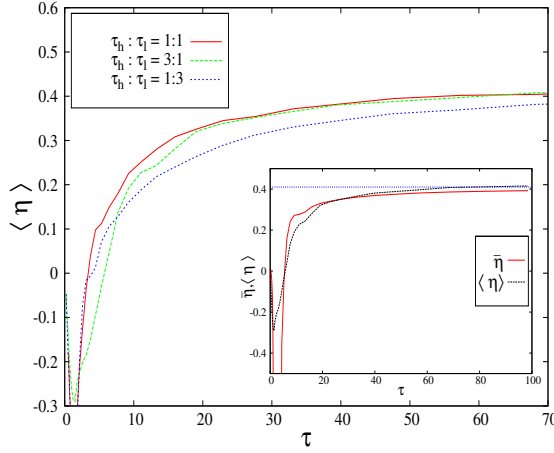


FIG. 15: (Color online) Variation of $\langle \eta \rangle$ vs τ for symmetric as well as asymmetrical cycles. inset: comparison of $\langle \eta \rangle$ with $\bar{\eta}$ for $\tau_h : \tau_l = 3 : 1$.

the quasistatic limit there should not be any effect of this asymmetry. This is clear from Fig.(14) that the average work, for three different asymmetric cycles, asymptotically approach each other in the quasistatic limit. In the non-quasistatic limit, work extracted by the engine for asymmetric cycles is small compared to symmetric cycle. From Fig.(15) it is seen that $\langle \eta \rangle$ is lower for asymmetrical cycles. The inset shows even in quasistatic limit $\langle \eta \rangle \neq \bar{\eta}$ for $\tau_h : \tau_l = 3 : 1$. We have verified separately that asymmetry also decreases the power. Thus asymmetry in the cycle degrades the performance characteristics of the engine.

We now briefly compare the nature of power and efficiency of our system when the confining potential is different. We have taken the confining po-

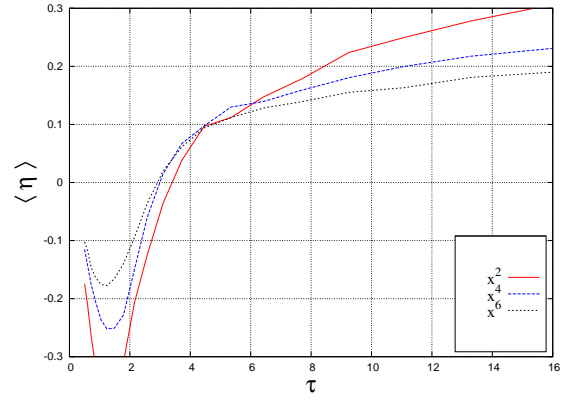


FIG. 16: (Color online) Variation of $\langle \eta \rangle$ with τ for different types of potentials.

tential $\frac{1}{2}k(t)x^n$ with $n=2,4,6$. For $n=4,6$ the confining potentials are referred to as hard potential. The equilibrium distributions for hard potentials are no longer Gaussian and hence in the quasistatic limit, the average work, heat dissipation etc., will be different from those for the harmonic potential.

In Fig.(16) and (17) we have plotted $\langle \eta \rangle$ and $\langle p \rangle$ as a function of cycle time for different potentials. Average efficiency $\langle \eta \rangle$ for large τ decreases as potential becomes harder and thereby degrading the performance. $\langle \eta \rangle$ saturates at the higher value of τ (not shown in the figure). From Fig.(17) we observe that harder the potential smaller will be the critical time τ above which the system acts as an engine. For large cycle time the power decreases as the potential becomes harder. However, we see clearly that there are three values of efficiencies $\langle \eta \rangle$ and $\bar{\eta}$ at maximum power 0.16, 0.10, 0.08 and 0.25, 0.16, 0.13 for $n=2,4,6$ respectively. It is apparent that the efficiency at maximum power is model dependent and decreases as the potential becomes harder. Even the saturation value is different and it is lower for harder potential. Clearly, these two figures indicate that operational characteristics of our system are model dependent. Thus we do not expect any universal relation involving only the average efficiency at maximum power and temperatures of the reservoirs.

So far we have studied our system in detail in the underdamped regime which is a general case. From now on we restrict to the overdamped regime and highlight some qualitative differences.

V. OVERDAMPED QUASISTATIC CASE

In the overdamped limit, dynamics of the system follows Langevin Eq.(2), where inertial effects are ignored. This approximation is valid when the

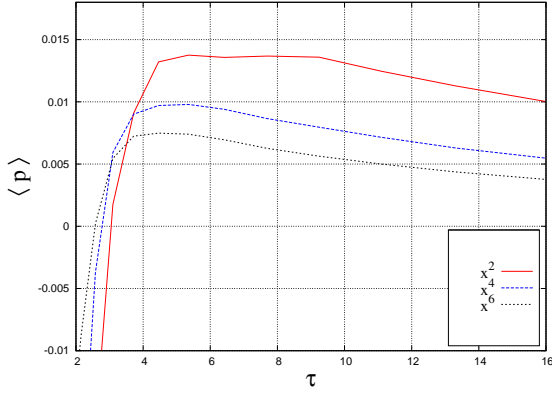


FIG. 17: (Color online) Variation of power $\langle p \rangle$ with τ for different types of potentials.

time steps of the observation are much larger than m/γ . The internal energy of the system is given only in terms of potential energy. For this case equilibrium distribution of a particle in a static harmonic potential is given by $P_{eq}(x) = Ne^{-\frac{kx^2}{2k_B T}}$ from which one can easily obtain the free energy. The analytical calculation for average thermodynamic quantities in quasistatic limit are similar to the underdamped case. The total average work done on the particle during the entire cycle is given by as

$$\begin{aligned} W_{tot} &= \Delta F_h + W_2 + \Delta F_l + W_4 \\ &= \frac{T_h}{2} \ln \frac{1}{2} - \frac{T_h}{4} + \frac{T_l}{2} \ln 2 + \frac{T_l}{2}. \end{aligned} \quad (21)$$

Interestingly, the expression for W_{tot} remains the same as for the case of the inertial system discussed earlier and the system extracts work provided $\frac{T_l}{T_h} < 0.705$. Using same arguments similar to the underdamped case and keeping in mind only the fact that there is only one phase space variable, namely position, the average internal energy change in the overdamped limit in the first step can be expressed as

$$\Delta U_1 = \frac{T_h}{2} - T_l. \quad (22)$$

Using the First law the average heat absorption from the hot bath during the first step is

$$-Q_1 = \Delta U_1 - \Delta F_h = \frac{T_h}{2} - T_l - \frac{T_h}{2} \ln \frac{1}{2}. \quad (23)$$

The expression for efficiency in the overdamped case is

$$\bar{\eta}_q = \frac{-W_{tot}}{-Q_1} = -\frac{\frac{T_h}{2} \ln \frac{1}{2} - \frac{T_h}{4} + \frac{T_l}{2} \ln 2 + \frac{T_l}{2}}{\frac{T_h}{2} - T_l - \frac{T_h}{2} \ln \frac{1}{2}}, \quad (24)$$

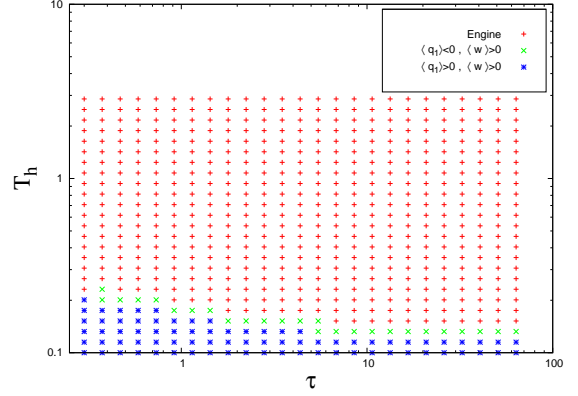


FIG. 18: (Color online) Phase diagram for different T_h and τ but for fixed $T_l = 0.1$.

which is different from the earlier case. In quasistatic limit, from Eq.(23) heat flows from the bath to the system provided $\frac{T_l}{T_h} < \frac{1+\ln 2}{2} = 0.846$. This ratio $\frac{T_l}{T_h}$ differs from that obtained for the underdamped case. From Eqs.(21) and (23), the system acts as an engine for the same condition ($\frac{T_l}{T_h} < 0.705$) as for the underdamped case. A finite temperature difference between hot and cold bath is required so that the system can act as a heat engine.

VI. FINITE CYCLE TIME ENGINE IN THE OVERDAMPED REGIME

Analysis for finite time cycle is carried out by numerical methods as discussed earlier. For a better understanding in the overdamped regime, all the parameters have been kept same as in the underdamped case. In Fig.(18), we have plotted the phase diagram for the overdamped case keeping T_l fixed at 0.1. For large τ (quasistatic limit) we observe, from phase diagram, that the system operates as a heat engine provided T_h is greater than a critical value. This critical value is close to the theoretical value of 0.142 obtained from the bounds determined in quasistatic calculation. The phase diagram shows a qualitative difference from the underdamped phase diagram (Fig.(3)). The system always acts as an engine in $\tau \rightarrow 0$ limit provided we are above a critical value of T_h , which is not the case for the underdamped engine. This is clear from Fig.(19), where we have plotted average work done on the system $\langle w \rangle$ and average heat released to each bath with $\langle q_1 \rangle$ and $\langle q_2 \rangle$ as a function of τ . Note that the observed anomalous part for $\langle w \rangle$ and $\langle q_1 \rangle$ in the underdamped case for small τ regime is absent in this regime. The quantities $\langle w \rangle$, $\langle q_1 \rangle$ and $\langle q_2 \rangle$ show monotonic behavior

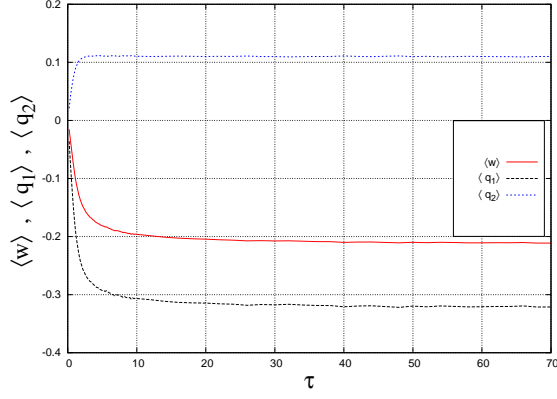


FIG. 19: (Color online) Variation of $\langle w \rangle$, $\langle q_1 \rangle$ and $\langle q_2 \rangle$ with cycle time τ .

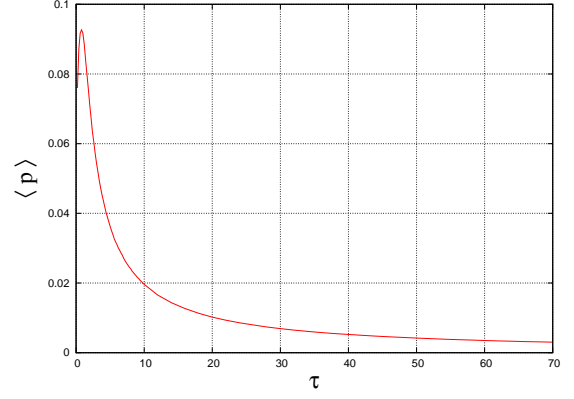


FIG. 21: (Color online) Variation of $\langle p \rangle$ with cycle time τ .

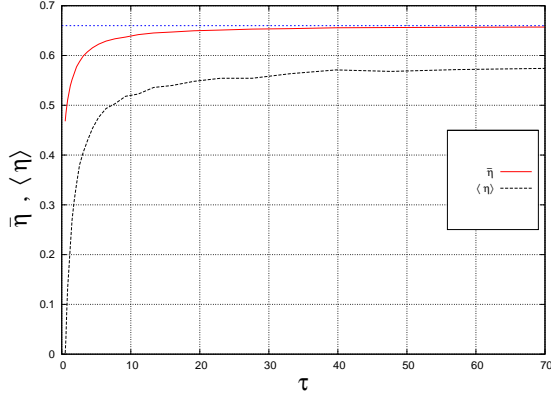


FIG. 20: (Color online) Variation of $\langle \eta \rangle$ and $\bar{\eta}$ with cycle time τ . The dotted blue line denotes the quasistatic limit for $\bar{\eta}$.

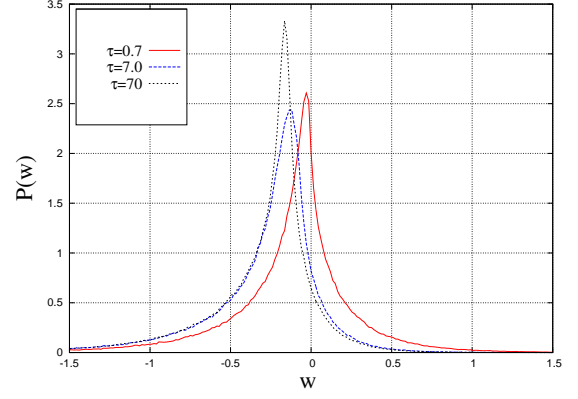


FIG. 22: (Color online) Distribution of w for different cycle times in the overdamped case.

and saturate at large cycle time to their analytical limits -0.214, -0.324 and 0.110, respectively. Unlike the underdamped case here, $\langle w \rangle$ and $\langle q_1 \rangle$ are always negative.

In Fig.(20) we have plotted the average of efficiency $\langle \eta \rangle$ and $\bar{\eta}$ as a function of τ . Both the efficiencies increase monotonically from zero and saturate for large τ . The saturation value of $\bar{\eta}$ is close to the theoretically predicted value of 0.660. The saturation value of $\langle \eta \rangle$ is found numerically to be 0.571 which is much less than the corresponding value of $\bar{\eta}$. Both these values are less than the Carnot value $\eta_c = 0.8$. It is clear that $\langle \eta \rangle \neq \bar{\eta}$ due to the strong correlation between fluctuating variables w and q_1 for all τ .

From Fig.(21), we see that power exhibits a sharp peak at $\tau = 0.8$. Corresponding efficiencies $\langle \eta \rangle$ and $\bar{\eta}$ at maximum power are equal to 0.11 and 0.51 which are less than the C-A result ($\eta_{CA} = 0.554$).

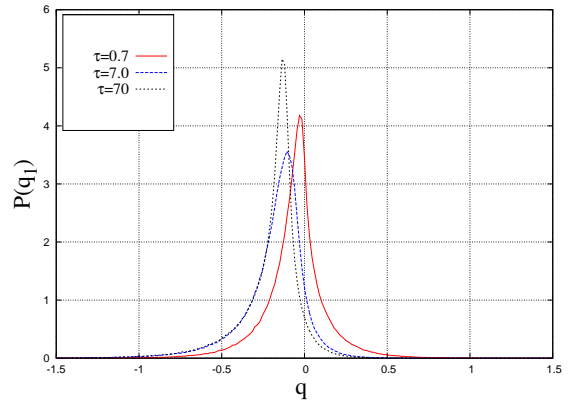


FIG. 23: (Color online) Distribution of q_1 for different cycle times in the overdamped case.

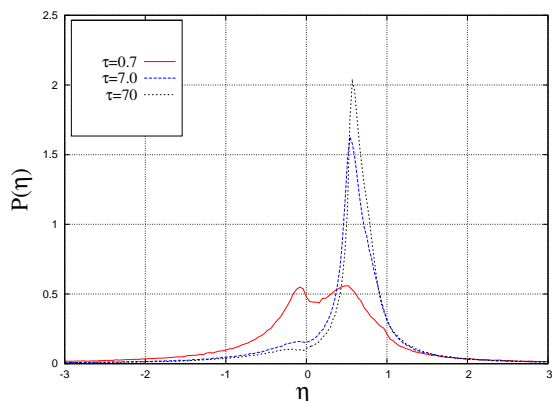


FIG. 24: (Color online) Distribution of η for different cycle times in the overdamped case.

To study the nature of fluctuations in the overdamped regime we have plotted the distribution $P(w)$, $P(q_1)$ and $P(\eta)$ in Figs.(22), (23) and (24) respectively. The qualitative nature of the distributions of $P(w)$ and $P(q_1)$ remain the same for different values of τ as in the underdamped case. The fluctuations are smaller compared to the underdamped case. The distribution $P(\eta)$ shows a double peak behavior for $\tau = 0.7$ with $\langle \eta \rangle = 0.086$ and standard deviation $\sigma_\eta = 1.688$. For $\tau = 7.0$, $\langle \eta \rangle = 0.496$ and $\sigma_\eta = 1.287$. For $\tau = 70$, $\langle \eta \rangle = 0.571$ and $\sigma_\eta = 1.234$. We observe that even in the quasistatic regime, fluctuations of η dominate over the mean value. Thus η is a non self averaging quantity. We have also seen that the fraction of the realizations for which the system acts as an engine, increases with cycle time τ . Numerical values for these fractions are 0.488, 0.817 and 0.861, for $\tau = 0.7$, 7.0 and 70.0, respectively. Hence, finite fraction of realization does not act as an engine even in quasistatic limit. Similar to the underdamped case, the reliability of the system to act as an engine increases with τ .

Finally, we discuss the performance characteristics of our system in the overdamped regime using an experimental protocol [8]. The experimental protocol consists of only two steps, in which the two adiabatic steps of Fig.(1) are absent. In the quasistatic regime the system acts as an engine for any temperature difference and there is no bound on T_h unlike our four step protocol [8]. This suggests that the phase diagram will depend on the nature of protocol as well as on system parameters and is not unique. As discussed earlier, most of the work fluctuations specially in quasistatic regime arise from two adiabatic steps. In the absence of these two steps, we have observed in our simulation that in the quasistatic regime, work distribution $P(w)$ is sharply peaked like a delta func-

tion at $W = -\frac{1}{2}(T_h - T_l) \ln 2$ (analytical result) [8]. However, fluctuations in q_1 persist even in the quasistatic regime as a result of the relaxation process that follows when the system, in contact with the cold bath, is brought in direct contact with high temperature reservoir. The distribution of stochastic efficiency $P(\eta)$ exhibits a qualitative differences. It has almost zero weight for $\eta < 0$ in large τ limit and shows a broad double peak feature which is confined in the region $0 < \eta < 1$. Beyond $\eta > 1$ a long tail is observed. For $\tau = 70$ we have numerically calculated $\langle \eta \rangle = 0.579$ and $\sigma_\eta = 0.903$. Even for this protocol we notice that fluctuations dominates over the mean value. The details of these results will be published elsewhere [33].

VII. SUMMARY

We summarise our results in this section. We have carried out an extensive analysis of a single particle stochastic heat engine by manipulating a Brownian particle in a harmonic trap with a periodically time dependent stiffness constant as a protocol. The cycle consists of two isothermal steps and two adiabatic steps similar to that of Carnot engine. The proposed model is studied taking into account both the inertial and overdamped Langevin equations. Thermodynamic quantities, defined over microscopic phase space trajectory of our system, fluctuate from one cycle of operation to another. Their magnitude depends on the trajectory of the particle during the cycle. This is done by using the methods of stochastic energetics. Average value of thermodynamic quantities and their distribution functions have been calculated numerically in TPSS. Analytical results of average thermodynamic quantities have been obtained in the quasistatic regime. These results are consistent with the corresponding numerical results. We have reported several new results which were not addressed in earlier literature.

The full phase diagram for operation of a system is given in both inertial and high friction regime. They differ from each other qualitatively. In both cases it is also shown that system acts as an engine provided the temperature difference is greater than a critical value (unlike Carnot engine). This critical value depends on system parameters and is consistent with analytical results in quasistatic limit. Moreover, for fixed bath temperatures and system parameters there should be a critical cycle time above which the system acts as an engine.

The mean of the stochastic efficiency is dominated by its fluctuations ($\langle \eta \rangle < \sigma_\eta$) even in quasistatic regime, making the efficiency a non-self averaging quantity. For such cases mean ceases to be

a good physical variable and one has to resort to the analysis for full probability distribution. This is one of our main result. We have also shown that $\bar{\eta} = \frac{\langle w \rangle}{\langle q_1 \rangle} \neq \langle \frac{w}{q_1} \rangle = \langle \eta \rangle$.

Our analysis of model dependence of finite cycle time clearly rules out any simple universal relation (e.g., $\eta_{CA} = 1 - \sqrt{\frac{T_c}{T_h}}$.) between efficiency at maximum power and temperature of the baths. Time asymmetric periodic protocol makes engine less efficient. Only in the quasistatic regime time asymmetry does not play any role.

For given cycle time there are several realizations which do not work as a heat engine. These are referred to as transient second law violating trajectories. Number of these realizations decreases as we increase τ . The fractions of realizations following second law with corresponding τ are reported earlier sections both in underdamped and overdamped regimes. Thus for large cycle time the reliability of the system working as an engine increases. Persistence of these realizations even in quasistatic regime can be attributed to the fluctuation of heat and work distributions. Fluctuations in work are mainly attributed to two adi-

abatic processes connecting two isotherms, while fluctuations of q_1 result from the relaxation of the system, when brought in direct contact with high temperature reservoir from low temperature bath.

We have shown that in TPSS $P_{ss}(x, v, t)$ exhibit strong correlation between variables x and v in small cycle time limit. However, it becomes uncorrelated as we approach quasistatic limit. For analytical simplicity it had been generally assumed in earlier literature that there is no correlation between x and v in $P_{ss}(x, v, t)$ (see for example [16]).

In the inertial regime we have also verified the recently proposed fluctuation theorems for heat engines in a TPSS. Our results are amenable to experimental verifications.

VIII. ACKNOWLEDGMENTS

A.M.J. thanks DST, India for financial support and. A.S. thanks MPIPKS, Germany for partial support.

-
- [1] H. B. Callen, Thermodynamics and an Introduction to Thermostatistics (John Wiley & Sons, 2006).
 - [2] F. L. Curzon and B. Ahlborn, Am. J. Phys. **43**, 22 (1975).
 - [3] U. Seifert, Rep. Prog. Phys. **75**, 126001 (2012) and references therein.
 - [4] T. Schmiedl and U. Seifert, Europhys. Lett. **81**, 20003 (2008).
 - [5] C. Van den Broeck, Phys. Rev. Lett. **95**, 190602 (2005).
 - [6] M. Esposito, R. Kawai, K. Lindenberg and C. Van den Broeck, Phys. Rev. Lett. **105**, 150603 (2010).
 - [7] S. Sheng and Z. C. Tu, arXiv: 1404.7008.
 - [8] V. Blickle and C. Bechinger, Nature Phys. **8**, 143 (2012).
 - [9] C. Bustamante, J. Liphardt and F. Ritort, Phys. Today **58**, 43 (2005).
 - [10] K. Sekimoto, Stochastic Energetics (Springer, 2010).
 - [11] K. Sekimoto, Prog. Theor. Phys. Suppl. **130**, 17 (1998).
 - [12] D. Dan and A. M. Jayannavar, Physica A. **345**, 404 (2005).
 - [13] S. Saikia, R. Roy and A. M. Jayannavar. Phys. Lett. A. **369**, 367 (2007).
 - [14] P. Jop, A. Petrosyan and S. Ciliberto. Europhys. Lett. **81**, 50005 (2008).
 - [15] J. Hoppenau, M. Niemann, and A. Engel, Phys. Rev. E **87**, 062127 (2013).
 - [16] Z. C. Tu, Phys. Rev. E **89**, 052148 (2014)
 - [17] V. Holubec, arXiv: 1404.2030.
 - [18] G. Verley, T. Willaert, C. Van den Broeck and M. Esposito, arXiv:1404.3095.
 - [19] N. A. Sinitsyn J. Phys. A **44**, 405001 (2011).
 - [20] S. Lahiri, S. Rana, A. M. Jayannavar, J. Phys. A **45**, 465001 (2012).
 - [21] M. Campisi, J. Phys. A **47**, 245001 (2014).
 - [22] H. Risken, The Fokker-Planck Equation: Methods of Solution and Applications (Springer 1996).
 - [23] W. T. Coffey, Yu. P. Kalmykov and J. T. Waldorn, The Langevin Equation (World Scientific 2004).
 - [24] R. Mannela, in: J.A. Freund and T. Poschel (Eds), Stochastic Process in Physics, Chemistry and Biology, Lecture Notes in Physics, vol. 557 Springer-Verlag, Berlin(2000) p353.
 - [25] E. Boksenbojm, B. Wynants and C. Jarzynski, Physica A. **389**, 4406 (2010).
 - [26] F. Ritort, Poincare seminar **2**, 193 (2003).
 - [27] G. M. Wang, E. M. Sevick, E. Mittag, D. J. Searles, and D. J. Evans, Phys. Rev. Lett. **89**, 050601 (2002).
 - [28] M. Sahoo, S. Lahiri, A. M. Jayannavar, J. Phys. A **44**, 205001 (2011).
 - [29] U. Seifert, Phys. Rev. Lett. **95**, 040602 (2005).
 - [30] U. Seifert, Eur. Phys. J. B **64**, 423 (2008).
 - [31] S. Lahiri and A. M. Jayannavar Eur. Phys. J. B **69**, 87 (2009)
 - [32] A. Saha, S. Lahiri and A. M. Jayannavar, Phys. Rev. E **80**, 011117 (2009).
 - [33] S.R., P.S.P., A.S. and A.M.J. to be published